Structural basis of the mechanism of β-methyl epimerization by enzyme MarH

Bin Liu,[a,e,‡] Yan Hou,[c,‡] Xiaozheng Wang,[d] Xiaofang Ma,[a,e] Shiqi Fang,[a,e] Tao Huang,[a,e] Yanli Chen,[a] Zhiqiang Bai,[a,e] Shuangjun Lin,[d,*] Rundong Zhang[c,*] and Kaifeng Hu[a,b,*]

a Key Laboratory of Phytochemistry and Plant Resources in West China, Kunming Institute of Botany, Chinese Academy of Sciences, Kunming, Yunnan 650201, China

b Innovative Institute of Chinese Medicine and Pharmacy, Chengdu University of Traditional Chinese Medicine, Chengdu, Sichuan 611137, China.

c Department of Ophthalmology, State Key Laboratory of Biotherapy, West China Hospital, Sichuan University and Collaborative Innovation Center for Biotherapy, Chengdu, Sichuan, 610041, China

d State Key Laboratory of Microbial Metabolism, School of Life Sciences & Biotechnology, Shanghai Jiao Tong University, Shanghai, 200240, China

e University of Chinese Academy of Sciences, Beijing, 100049, China

Table of contents

Figures

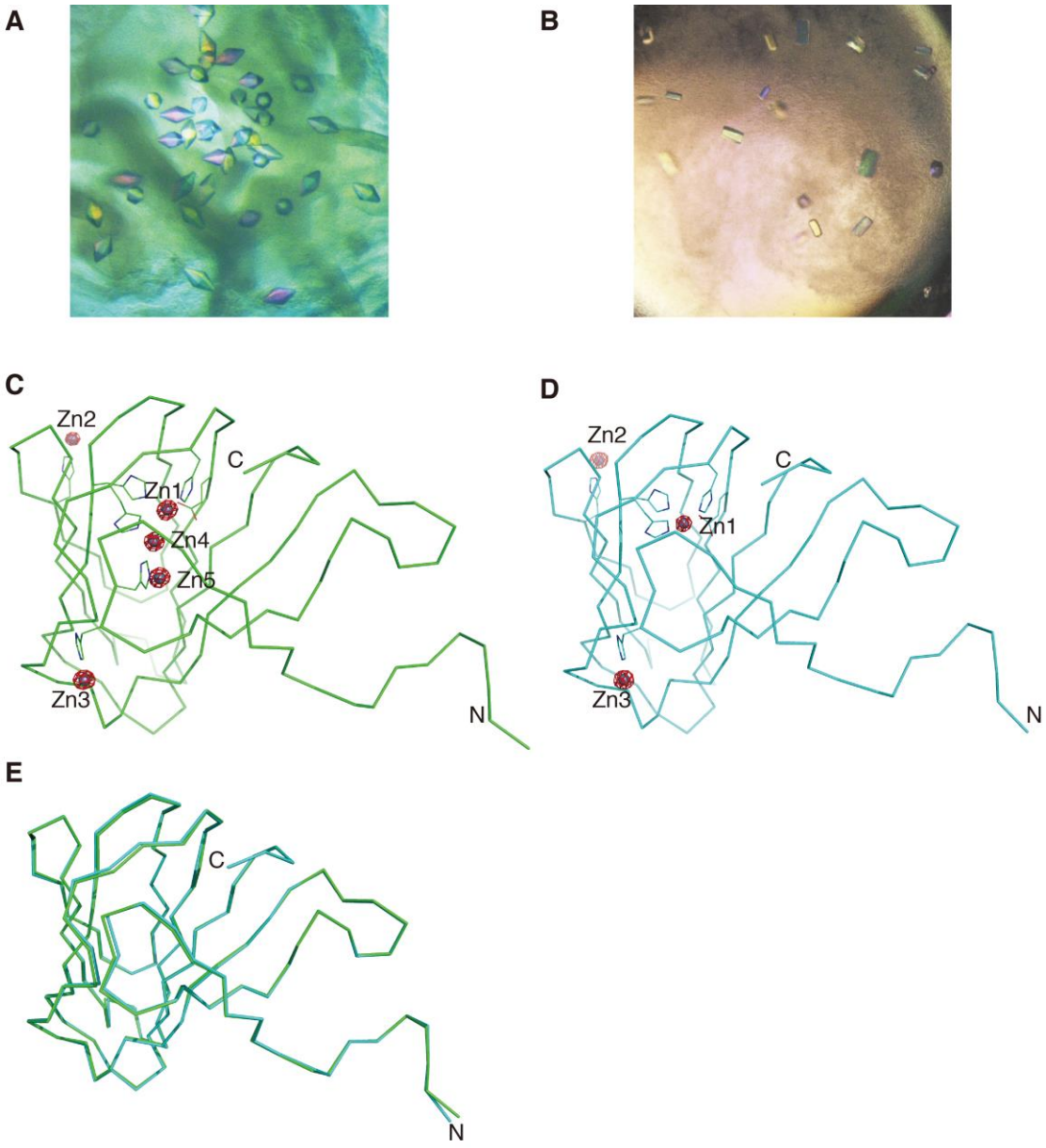

Figure S1. Two types of MarH crystals and their structures.
(A) and (B) Crystals of MarH grown in the presence of 0.4 M zinc acetate, 100 mM HEPES, pH 7.5, and 4% PEG3350 and in the presence of 10 mM $ZnSO_4$, 100 mM MES, pH 6.5, and 24% PEG550. (C) and (D) Monomeric structures of dimeric MarH in the asymmetric unit corresponding to crystallization conditions (A) (structure in green with 5 Zn atoms shown with their electron density contour highlighted in red) and (B) (structure in blue with 3 Zn atoms shown with their electron density contour highlighted in red). The electron density was calculated as an omit map contoured at 9.0 σ. (E) Superposition of the structures of MarH represented in (C) and (D). All structures are represented as ribbons.

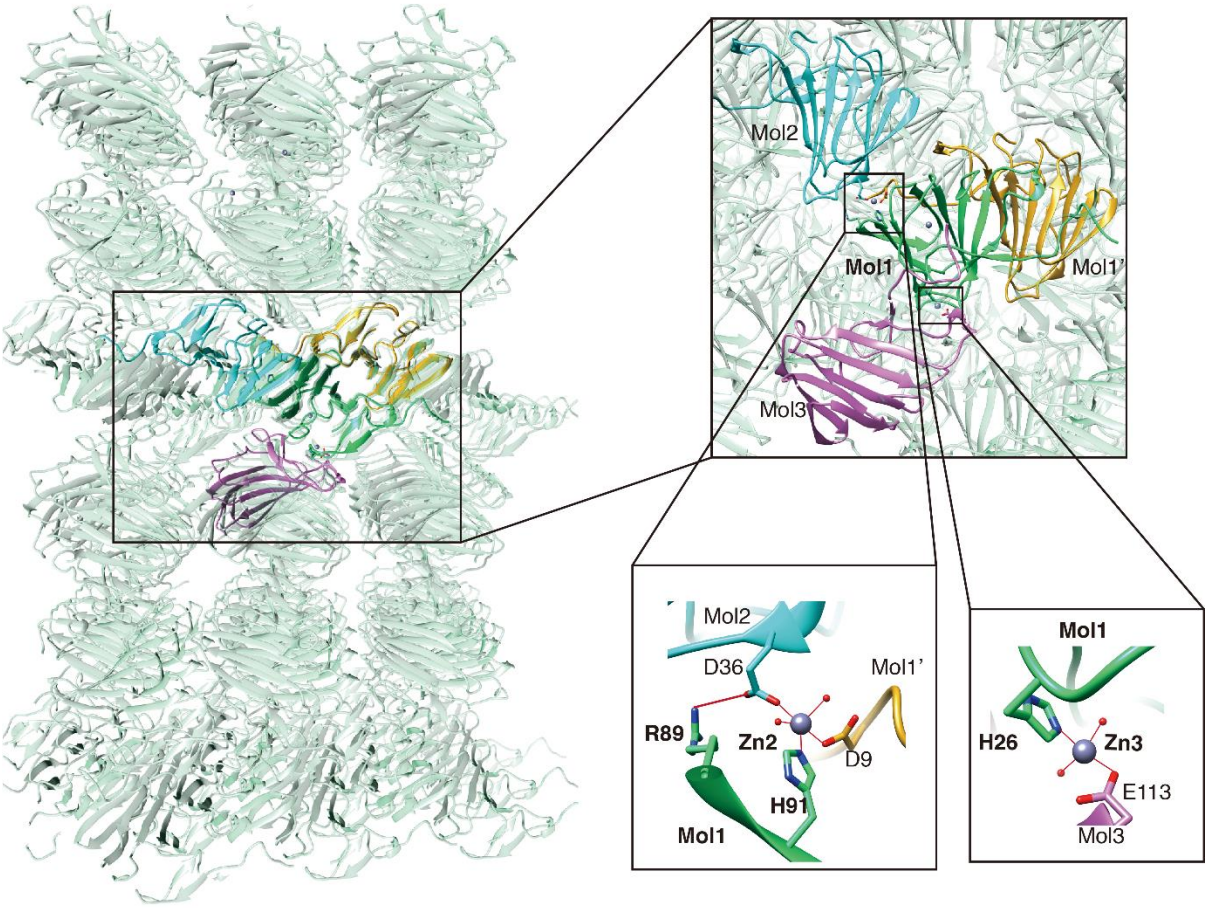

Figure S2. Crystal packing interactions.
Mo1, Mol1', Mol2 and Mol3 represent the monomers of MarH in the supercell. Mol1 and Mol1' are the subunits of a dimer. The amino acids and Zn ions belonging to Mol1 are indicated by bold text. The Zn-mediated crystal packing interactions of MarH under crystallization conditions with a low concentration of Zn: there is 1 Zn atom, Zn1, inside the molecule, while the crystal packing interactions are mediated by Zn2 and Zn3 on the surface of Mol1. The Zn-mediated crystal packing interactions of MarH under crystallization conditions with a high concentration of Zn are similar, i.e., mediated by Zn2 and Zn3 on the surface (not shown), but there are three Zn atoms inside the molecule (Figure S1C).

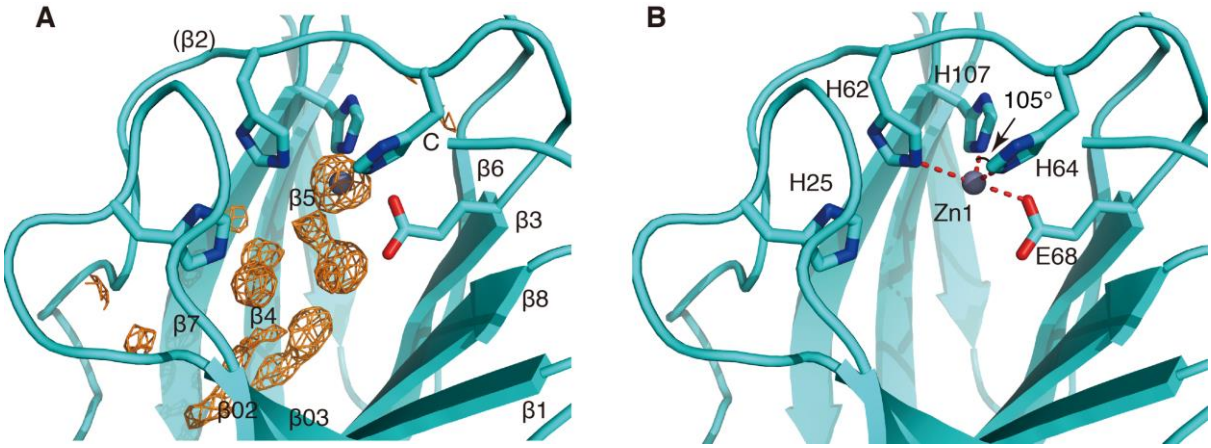

Figure S3. The bonding interactions at the metal ion coordination center of the MarH crystal structure grown with a low concentration of Zn.

The electron density (A) and detailed interactions (B) between the protein residues and Zn1 in the binding pocket of MarH grown with a low concentration of Zn (10 mM ZnSO4). The angles of His62(Nε2)-Zn-Glu(O) and His64(Nε2)-Zn-His107(Nε2) were measured to be 180° and 105°, respectively, suggesting a trigonal bipyramidal coordination geometry of Zn. The electron density inside the active pocket was calculated as an omit map contoured at 3.0 σ, and the detailed interactions between the protein residues and ions and small compounds are shown with red dashed lines.

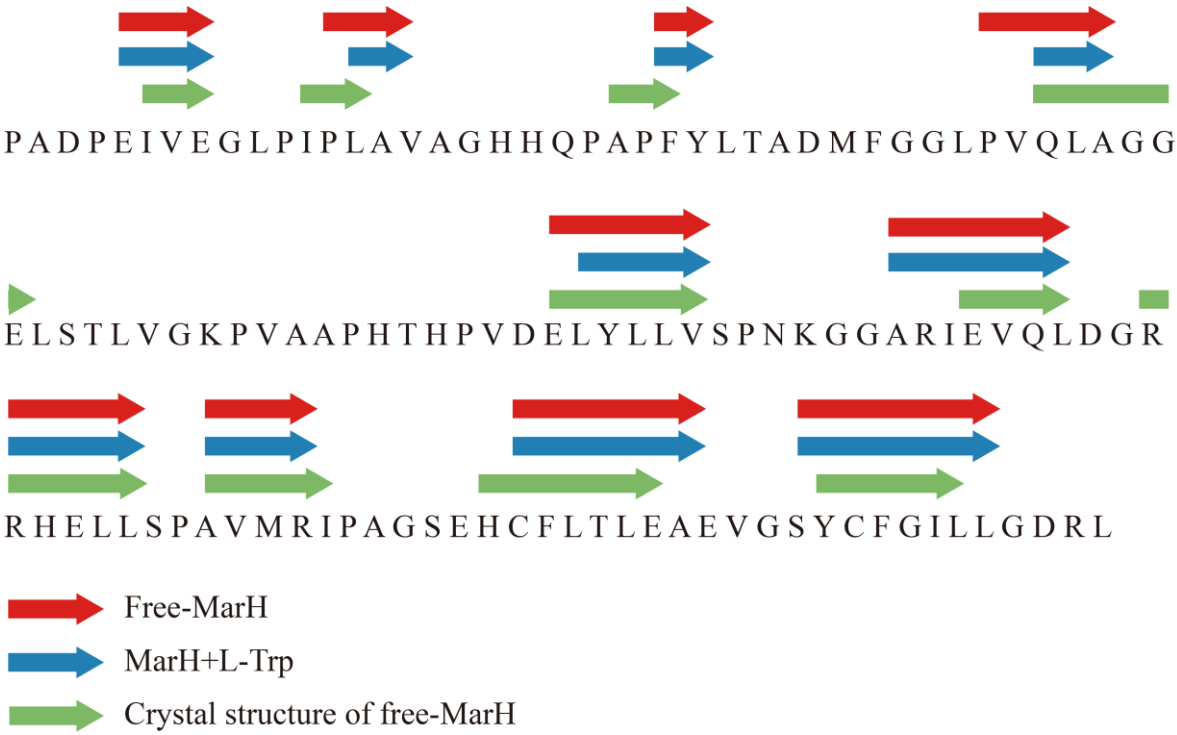

Figure S4. The predicted secondary structures were highly consistent with the secondary structural elements in the crystal structures.

Comparison of the secondary structures of MarH in the absence (red) and presence of substrate analogue L-Trp (blue) predicted by TALOS+ using the assigned backbone chemical shifts with the secondary structural elements in the crystal structure of free MarH (green). The β-sheets are represented by arrows. All structures have essentially unchanged secondary structural elements.

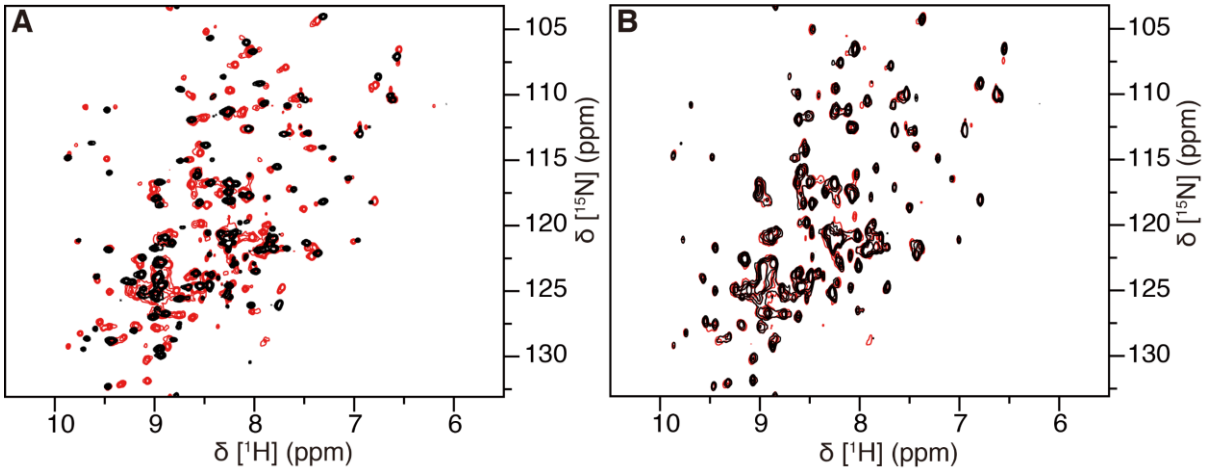

Figure S5. The E65A mutant is unable to bind the substrate analog, L-Trp.
(A) Comparison of the MarH E68A mutant (red) and wild-type MarH (black). The chemical shifts of the mutant are systematically different from those of the wild type, indicating that the mutation of Glu65 to Ala may induce a conformational change. (B) The ^{1}H-^{15}N HSQC spectra of MarH E65A in the absence (black) and presence (red) of L-Trp at a molar ratio of 1:2. No chemical shift perturbation was observed, suggesting that there is no interaction between L-Trp and the MarH E65A mutant.

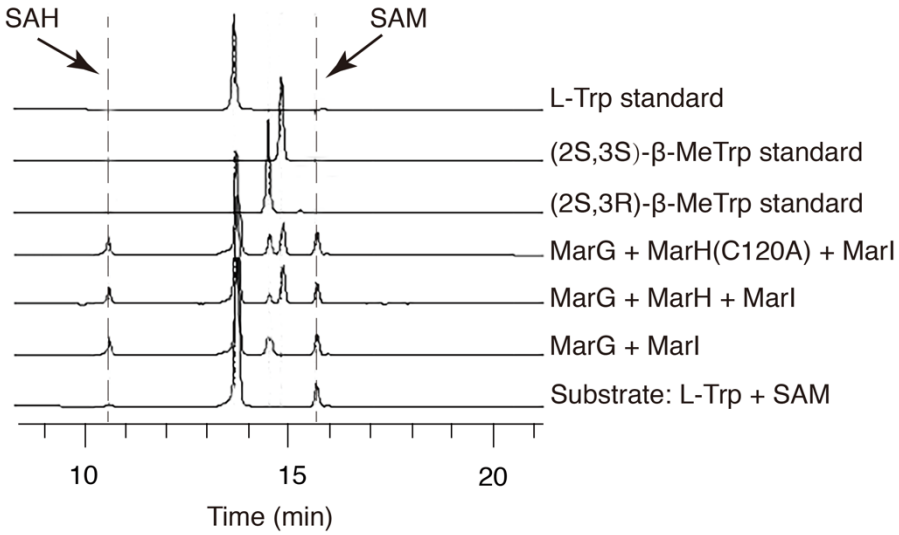

Figure S6. HPLC chromatograms (UV 280 nm) of MarG/I together with MarH- or MarH mutant-catalyzed reactions.

The MarH C120A mutant shows slightly decreased activity but is not completely inactive. SAM: *S*-adenosyl-L-methionine, SAH: *S*-adenosyl-L-homocysteine.

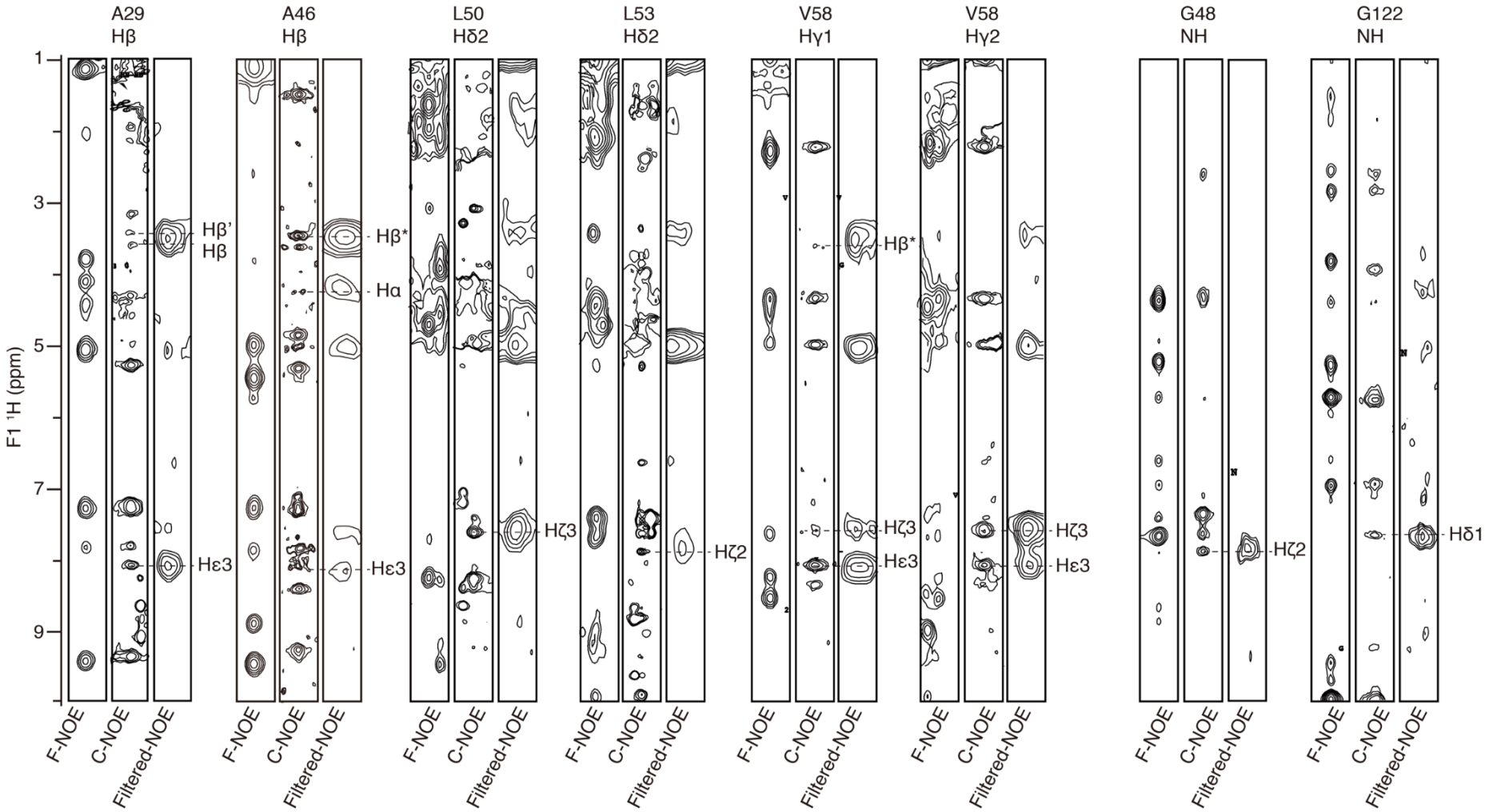

Figure S7. Assignments of the intermolecular NOEs.

The intermolecular NOEs between MarH and L-Trp were assigned by comparison of the ^{13}C-/^{15}N- resolved 3D NOESY spectra of ^{13}C,^{15}N-labeled MarH with (C-NOE) and without (F-NOE) the substrate analogue, L-Trp, and were further confirmed by the ^{13}C-/^{15}N- resolved ^{13}C,^{15}N-filtered 3D NOESY (Filtered-NOE) spectrum of the complex.

Tables

Table S1: Structural statistics for the ensemble of 20 complex structures[a]

Protein-ligand interface	
NOE distance constraints	
Intra-molecular NOE of involved active residues[b]	28
Protein-Ligand inter-molecular NOE	15
Average rmsd from the mean structure[c] (Å)	
active residues[b]	
all heavy atoms	1.014

[a] Statistical analysis was performed on the 20 structures with the lowest energy out of the total 200 calculated structures. [b] The residues assigned in the filtered NOE were defined as active residues. [c] Obtained by averaging the coordinates of the 20 ensemble structures, superposed using backbone atoms excluding the active residues.

Table S2. X-ray diffraction data collection and refinement statistics.

Values in parentheses are for the highest shell

Data	**Crystal A**				**Crystal B**
	remote	peak	Inflection 1	Inflection 2	
Wavelength (Å)	0.9787	1.28258	1.28364	1.28524	0.9787
Space group	$P3_121$ or $P3_221$	$P3_121$ or $P3_221$	$P3_121$ or $P3_221$	$P3_121$ or $P3_221$	$P3_121$ or $P3_221$
Unit cell (Å):	43.63,	43.63,	43.63,	43.63,	43.53,
a, b, c	43.63,	43.63,	43.63,	43.63,	43.53,
	99.97	99.97	99.97	99.97	98.14
Resolution range(Å)	50.0-1.58	50.0-2.07	50.0-2.07	50.0-2.07	50.0-1.58
	(1.61-1.58)	(2.11-2.07)	(2.11-2.07)	(2.11-2.07)	(1.61-1.58)
Unique reflections	15724	7208	7185	7236	15498
Completeness (%)	99.9 (100.0)	99.9(100.0)	99.9 (99.4)	99.6(95.1)	99.9(99.7)
R_{meas}	0.059 (0.095)	0.080(0.198)	0.089(0.199)	0.055(0.107)	0.062(0.379)
R_{pim}	0.013 (0.021)	0.019(0.046)	0.021(0.047)	0.013(0.026)	0.014(0.089)
Mean I/σ	49.0 (35.6)	39.2(25.0)	35.8(26.7)	53.0(25.7)	48.9(11.4)
Redundancy	19.1 (19.4)	18.2 (17.8)	18.1(17.4)	18.2 (16.6)	18.6(18.0)
Refinement Statistics					
Resolution range(Å)	37.8-1.58				35.2-1.58
R factor (%)	14.6				16.8
R_{free} factor (%)	17.7				20.8
Number of reflections	14901				14416
Number of atoms					
Rmsd bond length (Å)	0.0248				0.0263
Rmsd bond angles (°)	2.1579				2.5606
Ramachandran plot (%)[#]					
Favored,	97.52,				97.52,
additional allowed,	2.48,				2.48,
disallowed	0				0
PDB code	6J4B				6J4C

[#] gained from Coot program.

Table S3. The top 30 cupin-fold structures similar to MarH generated by DALI server against PDB90 representatives.

No.	PDB Code-Chain	Z	rmsd	lali	nres	%id	MOLECULE **in PDB Description**
1	2b8m-A	10.4	2.4	94	109	11	MOLECULE: HYPOTHETICAL PROTEIN MJ0764;
2	3rns-A	10.3	4.5	89	208	16	MOLECULE: CUPIN 2 CONSERVED BARREL DOMAIN PROTEIN;
3	5j4g-A	10.2	2.9	88	99	15	MOLECULE: UNCHARACTERIZED PROTEIN;
4	5fq0-A	10.2	3.0	93	110	18	MOLECULE: KDGF;
5	1yhf-A	10.0	2.6	91	114	15	MOLECULE: HYPOTHETICAL PROTEIN SPY1581;
6	3fjs-C	9.9	3.1	89	107	13	MOLECULE: UNCHARACTERIZED PROTEIN WITH RMLC-LIKE CUPIN FOLD
7	5fpz-A	9.9	2.8	94	110	16	MOLECULE: PECTIN DEGRADATION PROTEIN;
8	2ozj-A	9.8	3.6	87	110	20	MOLECULE: CUPIN 2, CONSERVED BARREL;
9	1v70-A	9.7	3.0	91	105	15	MOLECULE: PROBABLE ANTIBIOTICS SYNTHESIS PROTEIN;
10	6cb4-A	9.7	2.6	103	361	15	MOLECULE: CANAVALIN;
11	2oa2-A	9.6	3.1	91	132	18	MOLECULE: BH2720 PROTEIN;
12	2pfw-A	9.6	2.8	95	112	13	MOLECULE: CUPIN 2, CONSERVED BARREL DOMAIN PROTEIN;
13	5j7m-A	9.6	3.2	101	122	14	MOLECULE: CUPIN 2 CONSERVED BARREL DOMAIN PROTEIN;
14	2q30-D	9.5	2.8	90	106	10	MOLECULE: UNCHARACTERIZED PROTEIN;
15	3cew-A	9.5	2.9	92	118	17	MOLECULE: UNCHARACTERIZED CUPIN PROTEIN;
16	5e1r-C	9.5	2.9	105	358	12	MOLECULE: 7S VICILIN;
17	5wsd-A	9.5	3.3	99	118	7	MOLECULE: UNCHARACTERIZED PROTEIN TM1459;
18	5fzi-A	9.5	2.6	88	461	6	MOLECULE: LYSINE-SPECIFIC DEMETHYLASE 5B;
19	3h8u-A	9.4	3.1	99	121	11	MOLECULE: UNCHARACTERIZED CONSERVED PROTEIN WITH DOUBLE-STR
20	1o4t-A	9.4	2.9	99	115	13	MOLECULE: PUTATIVE OXALATE DECARBOXYLASE;
21	3h50-A	9.4	3.1	94	114	16	MOLECULE: TETRACENOMYCIN POLYKETIDE SYNTHESIS PROTEIN;
22	5vf5-A	9.4	2.5	102	370	14	MOLECULE: SM80.1 VICILIN;
23	2e9q-A	9.4	3.0	100	385	13	MOLECULE: 11S GLOBULIN SUBUNIT BETA;
24	2h0v-A	9.3	2.8	102	335	19	MOLECULE: QUERCETIN 2,3-DIOXYGENASE;
25	2phl-C	9.2	3.5	99	361	17	MOLECULE: PHASEOLIN;
26	2vpv-A	9.1	2.2	87	94	10	MOLECULE: PROTEIN MIF2;
27	2ea7-A	9.1	3.1	105	390	15	MOLECULE: 7S GLOBULIN-1;
28	4mv2-A	9.1	2.9	98	121	14	MOLECULE: PLU4264;
29	5fwj-A	9.1	2.5	84	436	7	MOLECULE: HISTONE DEMETHYLASE JARID1C;
30	2pyt-A	9.1	3.1	99	128	14	MOLECULE: ETHANOLAMINE UTILIZATION PROTEIN EUTQ;